3-1966

Stage-Fall-Discharge Relations For Flood Flows Over Highway Embankments

Gaylord V. Skogerboe

M. Leon Hyatt

Lloyd H. Austin

STAGE-FALL-DISCHARGE RELATIONS FOR FLOOD FLOWS OVER HIGHWAY EMBANKMENTS

Prepared by

Gaylord V. Skogerboe
M. Leon Hyatt
Lloyd H. Austin

Utah Water Research Laboratory
College of Engineering
Utah State University
Logan, Utah

March 1966 Report PR-WR6-7

ACKNOWLEDGMENTS

The authors wish to acknowledge that the information used in this report was taken from the U. S. Geological Survey Water-Supply Paper 1617-A, "Discharge Characteristics of Embankment-Shaped Weirs," which was prepared by Carl E. Kindsvater. Utilizing the data contained in the USGS paper, the method of submerged flow analysis developed at Utah State University for trapezoidal, flat-bottomed rectangular, and Parshall flumes is shown in this report to be valid as well for embankments. The data collected under the guidance of Mr. Kindsvater at the Georgia Institute of Technology has proven to be very accurate and reflects the quality of the experimental design and procedures.

TABLE OF CONTENTS

LIST OF TABLES

LIST OF FIGURES

NOMENCLATURE

Symbol	Definition
A	Area
b_1	Bottom width of rectangular flume at entrance section
b_2	Bottom width of rectangular flume in throat section
B	Contraction ratio, b_2/b_1
C	Coefficient in free flow equation
C_1	Coefficient in numerator of submerged flow equation
C_2	Coefficient in denominator of submerged flow equation
F	Force
g	Acceleration due to gravity
h	Upstream depth of flow measured from the elevation of the crown line
H_1	Total energy head at upstream section measured from the crown line elevation
L	Total width of the roadway (pavement plus two shoulders)
L_p	Pavement width
L_s	Shoulder width
n_1	Exponent in the free flow equation and numerator of the submerged flow equation
n_2	Exponent in the denominator of the submerged flow equation
P	Total height of the embankment
q	Discharge per foot of length of embankment
Q	Total flow rate, or discharge
S	Submergence, which is the ratio of a downstream depth to an upstream depth with both depths referenced to a common elevation

NOMENCLATURE (Continued)

Symbol	Definition
S_e	Embankment slope
S_p	Pavement cross slope
S_s	Shoulder slope
S_t	Transition or incipient submergence
t	Downstream depth of flow measured from the crown line elevation
V	Average velocity
V_1	Average velocity at section 1
V_2	Average velocity at section 2
y	Flow depth
y_1	Flow depth at section 1
y_2	Flow depth at section 2
y_c	Critical depth of flow
y_o	Flow depth at crown line
β	Momentum correction coefficient
γ	Specific weight of fluid
λ	Embankment slope
ρ	Density of fluid
f(S)	Defined by $1/(-\log S)$
$\phi_m(S)$	Defined by $1/\sqrt{(1 - S)^3/S(1 + S)}$

SCOPE OF STUDY

At Utah State University, considerable effort has been devoted to the analysis of submerged flow at open channel constrictions. A method of analyzing submerged flow was first developed for a trapezoidal flume by Hyatt (1965). Later studies verified the method of analysis for a rectangular flume (Skogerboe, Walker, and Robinson, 1965) and Parshall flumes (Skogerboe, Hyatt, England, and Johnson, 1965). Because of previous findings, it was felt this method of analyzing submerged flow could be applied to highway embankments.

A highway embankment is a form of broad-crested weir when overtopped by flood waters. Being a weir, the flood discharge over the embankment is only a function of the upstream depth for free flow conditions. This report will present a method for determining the discharge under submerged flow conditions using the upstream and downstream depths. Thus, postflood field measurements and observations, when properly obtained, will provide the necessary information for an accurate determination of the flood discharge for either free or submerged flow conditions.

The concepts involved in the analysis of submerged flow at open channel constrictions were originally developed by dimensional analysis for flow measuring flumes. The parameters describing submerged flow in flumes have been further verified by the development of theoretical submerged flow equations which utilize momentum theory and energy relationships.

The experimental models studied by Kindsvater (1964) are comparable to a secondary highway embankment. The models were constructed to a scale of 1/9 a typical secondary roadway. The data resulting from the model studies has been subjected to the method of submerged flow analysis previously employed with flow measuring flumes. The consistency of the data, both for free flow and submerged flow, reflects the quality of the experimental design and procedures employed in collecting the data. Although the data presented in this report applies only to various forms of secondary road embankments, the methods of analysis are general. The development of calibration curves for other embankment geometries requires only the generation of additional data employing model studies.

FLOW REGIMES

The two most significant flow regimes or conditions are free flow and submerged flow. The distinguishing difference between the two is the fact that critical depth occurs on the roadway for the free flow condition, usually near the crown line. This critical-flow control on the roadway requires only the measurement of a depth upstream from the point of critical depth for determination of the discharge. When the downstream or tailwater depth is raised sufficiently, the flow depth at the crown line becomes greater than critical depth, and submerged flow conditions exist. With submerged flow, a change in the tailwater depth also affects the upstream depth and a rating for the embankment will

require that two flow depths be measured, one upstream and one downstream from the crown line. The flow condition at which the regime changes from free flow to submerged flow is a transition state, and the value of submergence at which this condition occurs is often referred to as the transition or incipient submergence. The authors prefer the designation of transition submergence symbolized by S_t. The transition from free to submerged flow is somewhat unstable and is difficult to produce in the laboratory.

Kindsvater (1964) subclassifies free flow into plunging flow and surface flow. Plunging flow occurs when the flow jet plunges under the tailwater surface resulting in a submerged hydraulic jump on the downstream face of the embankment slope. Surface flow is the condition which exists when the flow jet separates from the embankment surface at the downstream shoulder and "rides" over the tailwater surface. Hence, submerged flow is always a surface flow, but free flow can be either plunging flow or surface flow. Kindsvater (1964) further defines the upper limit of the free flow transition range as the change from plunging flow to surface flow when the tailwater depth is being raised. The lower limit of the free flow transition range is the change from surface flow to plunging flow when the tailwater depth is being lowered. Fig. 1 illustrates the various flow regimes explained above. Water surface profiles are drawn for a typical embankment with profile a designating submerged flow, profile b the transition or incipient submergence, profile c the upper limit of transition range (surface flow), profile d the lower limit

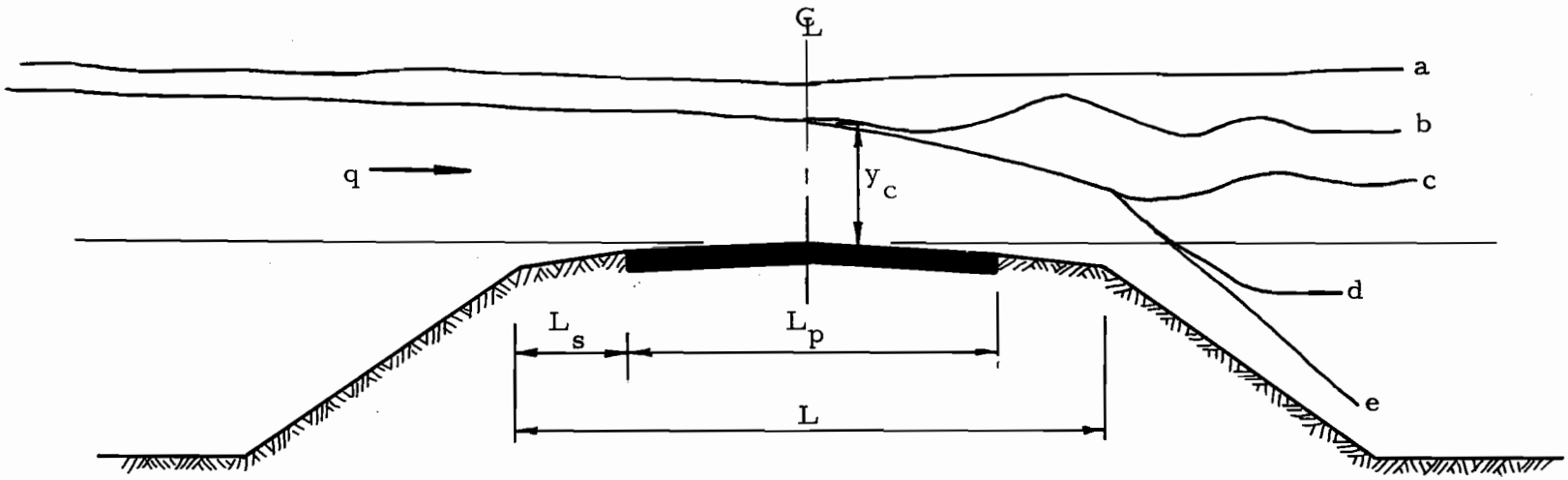

Fig. 1. Illustration of flow regimes over an embankment.

of transition range (plunging flow), and profile e free flow (plunging). The vertical scale in Fig. 1 is plotted 2.5 times larger than equivalent horizontal dimensions to better illustrate the various flow regimes. Despite this type of a breakdown in the flow regimes, it is to be noted that the upstream water depth remains unchanged for profiles b, c, d, and e, which are free flow surface profiles. However, as pointed out by Kindsvater (1964) the significance in the description of the various flow patterns in the free flow transition range is the determination of the embankment's safety against destructive erosion. The surface flows are much less erosive to the downstream embankment slope than the plunging flows.

CONCEPTS OF SUBMERGED FLOW AND FREE FLOW

Dimensional analysis was first applied to a trapezoidal flume (Hyatt, 1965) to develop the dimensionless parameters which describe submerged flow. The parameters which were found to describe submerged flow were: (1) the maximum Froude number occurring in the flume (which corresponds with the point of minimum depth of flow in the flume throat); (2) submergence, defined at the ratio of the tailwater depth to the upstream depth of flow; and (3) an energy loss parameter defined as the difference between the upstream depth and tailwater depth divided by the minimum depth of flow in the flume throat. A plot of the three parameters provides a unique relationship for any particular flume geometry. Manipulation of the equations relating the dimensionless

parameters yields a submerged flow discharge equation which is dependent upon only the upstream and downstream flow depths. The general form of the submerged flow equation can be expressed as

$$Q = \frac{C_1 (y_1 - y_2)^{n_1}}{[-(\log y_2/y_1 + C_2)]^{n_2}} \quad . \quad . \quad . \quad . \quad . \quad . \quad . \quad . \quad . \quad . \quad (1)$$

where y_1 and y_2 are flow depths measured upstream and downstream from the point of minimum flow depth, C_1 and C_2 are coefficients which depend upon the geometry of the structure, and n_1 and n_2 are exponents which are also related to the structure geometry. The calibration curves depicting this relationship are a family of curves obtained by plotting discharge, Q, as the ordinate, difference between upstream and downstream depths of flow, $y_1 - y_2$, as the abscissa, and submergence, y_2/y_1, as the varying parameter.

The free flow equation for flow measuring flumes can be expressed by

$$Q = C\, y_1^{n_1} \quad . \quad . \quad . \quad . \quad . \quad . \quad . \quad . \quad . \quad . \quad . \quad . \quad . \quad . \quad . \quad (2)$$

One noteworthy factor discovered from the flume studies (Skogerboe, Hyatt, England, and Johnson, 1965; and Skogerboe, Hyatt, Johnson, and England, 1965) is that the exponent on the $y_1 - y_2$ term in the submerged flow equation (Eq. 1) is identical to the exponent on the y_1 term in the free flow equation (Eq. 2) for any given flume.

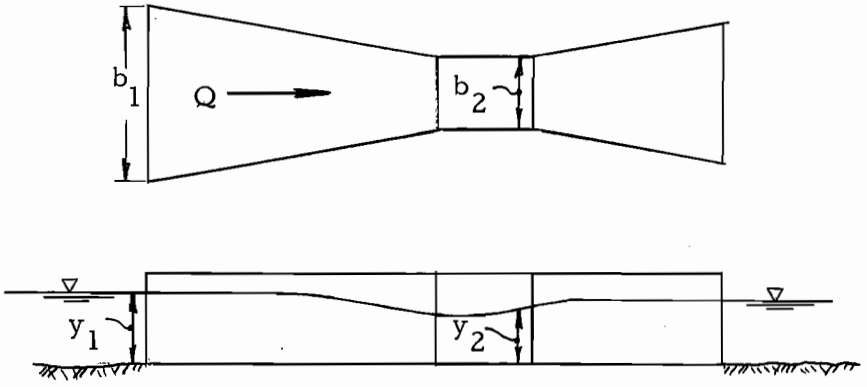

Fig. 2. Definition sketch for rectangular flat-bottomed flume.

The development of theoretical submerged flow equations are useful for further verification of the parameters used in the empirical submerged flow equation (Eq. 1). Theoretical equations will be listed for the rectangular flume illustrated above. Using the energy equation, and assuming steady frictionless flow, the following discharge equation can be developed

$$Q = \frac{(2g)^{1/2}\, b_2\, (y_1 - y_2)^{3/2}}{\sqrt{\dfrac{(1 - B^2S^2)\,(1 - S)^2}{S^2}}} \qquad (3)$$

where B is the contraction ratio, b_2/b_1, and S is the submergence, y_2/y_1. Employing momentum theory, and assuming steady frictionless flow with uniform velocity and hydrostatic pressure distributions, the following submerged flow discharge equation is developed

$$Q = \frac{(g/2)^{1/2} b_2 (y_1 - y_2)^{3/2}}{\sqrt{\frac{(1 - BS)(1 - S)^2}{S(1 + S)}}} \quad . \quad . \quad . \quad . \quad . \quad . \quad . \quad . \quad . \quad . \quad (4)$$

The real value of Eqs. 3 and 4 is the further verification of the format of the empirical submerged flow equation (Eq. 1). For any particular flume geometry, the contraction ratio, B, and the throat width, b_2, are constants. Consequently, the discharge in the theoretical submerged flow equations (Eqs. 3 and 4) becomes a function of $(y_1 - y_2)^{3/2}$ and the submergence, S. Therefore, the theoretical equations are similar in format to the empirical equation derived from dimensional analysis where the discharge is a function of $(y_1 - y_2)^{n_1}$ and the submergence, S.

For the problem at hand, flow over a highway embankment, a theoretical free flow equation can be developed by assuming one-dimensional, steady, frictionless flow with uniform velocity distribution and hydrostatic pressure distribution. The resulting equation, which is listed by Kindsvater, is

$$q = 2/3 (2g/3)^{1/2} H_1^{3/2} = 3.09 H_1^{3/2} \quad . \quad . \quad . \quad . \quad . \quad . \quad . \quad (5)$$

where H_1 is the total head (flow depth plus velocity head, $V^2/2g$). The similarity between Eqs. 2 and 5 should be noted. The free flow equations derived from Kindsvater's data have utilized the upstream flow depth, h, rather than the total head, H_1. Although not reported herein, free flow equations were developed using the total head which showed that the exponent of H_1 was different from 3/2.

The assumptions made in the development of the theoretical equations are not entirely valid and consequently do not represent the actual discharge that will occur at an open channel constriction. For example, the exponent of $y_1 - y_2$ for rectangular flumes is greater than 3/2. A theoretical discharge equation developed for an embankment-shaped weir would also contain the term $(y_1 - y_2)^{3/2}$, or using the terminology for embankments, $(h-t)^{3/2}$. As will be shown later, the exponent of $h-t$ in the empirical submerged flow equation is greater than 3/2.

MOMENTUM THEORY APPLIED TO EMBANKMENTS

Momentum theory can be applied to develop submerged flow discharge equations for embankment-shaped weirs. Such equations are useful and instructive for comparison with the empirical approach developed from dimensional analysis. A control volume of fluid will be used which is bounded by the vertical sections at 1 and 2, the water surface, and the surface of the embankment as shown in Fig. 3.

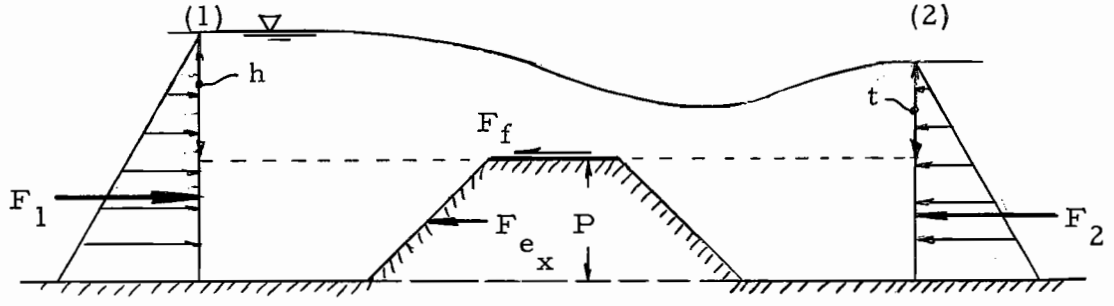

Fig. 3. Control volume for analysis of embankment-shaped weir.

A solution for the horizontal component of the form resistance force due to the embankment will be developed. A generalized diagram of the force of the embankment acting on the fluid is shown in Fig. 4.

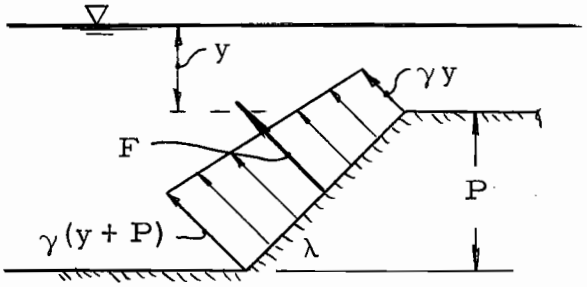

Fig. 4. Definition sketch for force acting on the fluid due to embankment.

$$F(\text{lb/ft}) = \left[\gamma y + \frac{\gamma(y + P) - \gamma y}{2}\right] \frac{P}{\sin \lambda}$$

$$= \frac{\gamma P}{\sin \lambda} \left(y + \frac{P}{2}\right) \quad . \quad . \quad . \quad . \quad . \quad . \quad . \quad . \quad . \quad . \quad . \quad (6)$$

$$F_x \text{ (lb/ft)} = \frac{\gamma P}{\sin \lambda} \left(y + \frac{P}{2}\right) \sin \lambda$$

$$= \gamma P \left(y + \frac{P}{2}\right) \quad . \quad . \quad . \quad . \quad . \quad . \quad . \quad . \quad . \quad . \quad . \quad (7)$$

The force of the embankment on the fluid will be designated as F_u for the upstream slope and F_d for the downstream slope. Assuming the pressure acting on the upstream slope of the embankment is hydrostatic and due to the water surface elevation at section 1, while the pressure acting on the downstream slope of the embankment is hydrostatic and due to the water surface elevation at section 2, the horizontal components of F_u and F_d can be developed from similarity with the equation for F_x (Eq. 7).

$$F_{u_x} = \gamma P (h + P/2) \quad (8)$$

$$F_{d_x} = \gamma P (t + P/2) \quad (9)$$

$$F_{e_x} = \gamma P (h + P/2) - \gamma P (t + P/2)$$

$$= \gamma P (h - t) \quad (10)$$

The forces acting on the control volume at sections 1 and 2 (Fig. 3) can be determined by assuming hydrostatic pressure distributions.

$$F_1 = \gamma (h + P)^2/2 \quad (11)$$

$$F_2 = \gamma (t + P)^2/2 \quad (12)$$

If friction losses are neglected ($F_f = 0$), the summation of forces in the horizontal direction can be evaluated.

$$\Sigma F_x = F_1 - F_2 - F_{e_x} \quad (13)$$

$$\Sigma F_x = \gamma (h + P)^2/2 - \gamma (t + P)^2/2 - \gamma P (h - t)$$

$$= \gamma (h^2 + 2Ph + P^2 - t^2 - 2Pt - P^2 - 2Ph + 2Pt)/2$$

$$= \gamma (h^2 - t^2)/2 \quad (14)$$

The same equation for the resultant horizontal force (Eq. 14) can be obtained using the simplified control volume shown in Fig. 5.

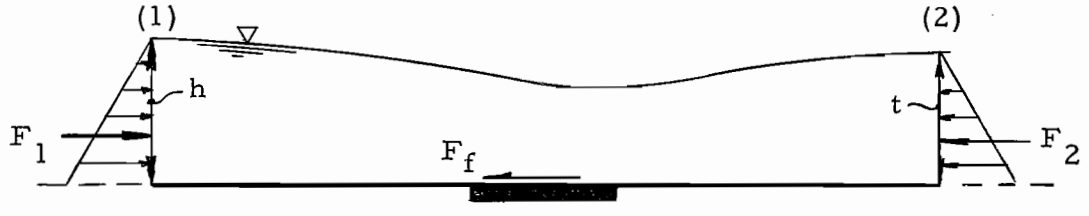

Fig. 5. Simplified control volume for analysis of embankment-shaped weir.

Hydrostatic pressure distributions will be assumed at sections 1 and 2.

$$F_1 = \gamma h^2/2 \quad . \quad . \quad . \quad . \quad . \quad . \quad . \quad . \quad . \quad . \quad . \quad . \quad . \quad (15)$$

$$F_2 = \gamma t^2/2 \quad . \quad . \quad . \quad . \quad . \quad . \quad . \quad . \quad . \quad . \quad . \quad . \quad . \quad (16)$$

Again, the friction forces will be neglected ($F_f = 0$).

$$\Sigma F = F_1 - F_2 \quad . \quad . \quad . \quad . \quad . \quad . \quad . \quad . \quad . \quad . \quad . \quad . \quad . \quad (17)$$

$$\Sigma F = \gamma h^2/2 - \gamma t^2/2$$

$$= \gamma (h^2 - t^2)/2 \quad . \quad . \quad . \quad . \quad . \quad . \quad . \quad . \quad . \quad . \quad . \quad . \quad (18)$$

Since Eqs. 14 and 18 are identical, two methods of analysis are suggested for deriving theoretical submerged flow discharge equations. A simplified analysis can be made using the control volume shown in Fig. 5 assuming uniform velocity distributions over the flow depths, h and t. A more general submerged flow equation can be derived using the control volume shown in Fig. 3 and assuming uniform velocity distributions over the upstream flow depth, h + P, and the downstream flow depth, t + P. The simplified analysis might be considered appropriate if the flow depths, h and t, were measured at the upstream edge and downstream edge of the embankment surface, respectively. The more general analysis requires that the flow depths, h and t, be measured at a sufficient distance upstream and downstream from the embankment in order for the assumption of uniform velocity distribution to be valid. Submerged flow equations will be developed for both methods of analysis.

Simplified Analysis

The analysis to follow is based on the control volume shown in Fig. 5. For the one-dimensional control volume, the momentum equation can be written as

$$\Sigma F = q\rho\,(\beta_2 V_2 - \beta_1 V_1) \quad . \quad . \quad . \quad . \quad . \quad . \quad . \quad . \quad . \quad . \quad (19)$$

Using Eq. 19 for the summation of forces, and assuming uniform velocity distributions at sections 1 and 2

$$\gamma h^2/2 - \gamma t^2/2 = q\rho\,(V_2 - V_1) \quad . \quad . \quad . \quad . \quad . \quad . \quad . \quad . \quad . \quad (20)$$

The continuity equation, $q = yV$, can be employed if steady flow is assumed.

$$\frac{\gamma h^2}{2} - \frac{\gamma t^2}{2} = \frac{q\gamma}{g}\left[\frac{q}{t} - \frac{q}{h}\right] \quad . \quad . \quad . \quad . \quad . \quad . \quad . \quad . \quad . \quad (21)$$

$$\frac{1}{2}\left[h^2 - t^2\right] = \frac{q^2}{g}\left[\frac{h-t}{th}\right]$$

$$q^2 = \frac{g\,th}{2}\,(h + t)$$

$$q = \frac{(g/2)^{1/2}}{\sqrt{\dfrac{1}{th\,(h+t)}}} \quad . \quad . \quad . \quad . \quad . \quad . \quad . \quad . \quad . \quad . \quad . \quad . \quad (22)$$

multiplying numerator and denominator by $(h - t)^{3/2}$

$$q = \frac{(g/2)^{1/2}\,(h-t)^{3/2}}{\sqrt{\dfrac{(h-t)^3}{th\,(h+t)} \cdot \dfrac{h^2}{h^2}}} \quad . \quad . \quad . \quad . \quad . \quad . \quad . \quad . \quad . \quad . \quad (23)$$

$$q = \frac{(g/2)^{1/2}\,(h-t)^{3/2}}{\sqrt{\dfrac{(1 - t/h)^3}{t/h\,(1 + t/h)}}} \quad . \quad . \quad . \quad . \quad . \quad . \quad . \quad . \quad . \quad . \quad (24)$$

Let the submergence, t/h, be represented by S.

$$q = \frac{(g/2)^{1/2} (h - t)^{3/2}}{\sqrt{\frac{(1 - S)^3}{S(1 + S)}}} \quad . \quad . \quad . \quad . \quad . \quad . \quad . \quad . \quad . \quad . \quad . \quad (25)$$

General Analysis

The following analysis is made using the control volume shown in Fig. 3. Assuming uniform velocity distributions at sections 1 and 2, the following momentum equation can be written.

$$\Sigma F_x = q\rho \ (V_2 - V_1) \quad . \quad . \quad . \quad . \quad . \quad . \quad . \quad . \quad . \quad . \quad . \quad (26)$$

The summation of horizontal forces is given by Eq. 14.

$$\gamma (h^2 - t^2)/2 = q\rho \ (V_2 - V_1) \quad . \quad . \quad . \quad . \quad . \quad . \quad . \quad . \quad . \quad . \quad (27)$$

Assuming steady flow, the continuity equation, $q = Vy$, can be employed.

$$q = V_1 (h + P) = V_2 (t + P) \quad . \quad . \quad . \quad . \quad . \quad . \quad . \quad . \quad . \quad . \quad (28)$$

The continuity equation can be substituted into Eq. 27.

$$\frac{\gamma (h^2 - t^2)}{2} = q \frac{\gamma}{g} \left[\frac{q}{t + P} - \frac{q}{h + P} \right] \quad . \quad . \quad . \quad . \quad . \quad . \quad . \quad (29)$$

$$\frac{g}{2} (h^2 - t^2) = q^2 \left[\frac{h - t}{(t + P)\ (h + P)} \right]$$

$$g (h + t) = q^2 \left[\frac{1}{(t + P)\ (h + P)} \right]$$

$$q = (g/2)^{1/2} \sqrt{(h + t)\ (t + P)\ (h + P)} \quad . \quad . \quad . \quad . \quad . \quad . \quad . \quad . \quad (30)$$

multiplying the right hand side by $(h - t)^{3/2} / (h - t)^{3/2}$

$$q = \frac{(g/2)^{1/2} (h - t)^{3/2}}{\sqrt{\frac{(h - t)^3}{(h + t)\ (t + P)\ (h + P)}}} \quad . \quad . \quad . \quad . \quad . \quad . \quad . \quad . \quad . \quad (31)$$

Multiplying the numerator and denominator inside the radical by h^3

$$q = \frac{(g/2)^{1/2} (h - t)^{3/2}}{\sqrt{\frac{(1 - t/h)^3 h^3}{(h + t)(t + P)(h + P)}}} \quad . \quad . \quad . \quad . \quad . \quad . \quad . \quad . \quad . \quad . \quad (32)$$

Let the submergence, t/h, be designated by S.

$$q = \frac{(g/2)^{1/2} (h - t)^{3/2}}{\sqrt{\frac{(1 - S)^3}{(1 + S)(S + P/h)(1 + P/h)}}} \quad . \quad . \quad . \quad . \quad . \quad . \quad . \quad . \quad . \quad (33)$$

when $P = 0$

$$q = \frac{(g/2)^{1/2} (h - t)^{3/2}}{\sqrt{\frac{(1 - S)^3}{(1 + S)S}}} \quad . \quad . \quad . \quad . \quad . \quad . \quad . \quad . \quad . \quad . \quad (34)$$

which is identical to the submerged flow equation developed from the simple analysis (Eq. 25).

Equation Characteristics

Although the assumptions made in the development of the theoretical submerged flow equations are not entirely valid, the equations do contain certain characteristics which can be compared with the submerged flow equation developed from dimensional analysis. In order to make a comparison between the two submerged flow equations (Eqs. 1 and 33), assume C_2 equal to zero in Eq. 1. This assumption will later prove to be valid for the embankment-shaped weirs under study. Define the denominator of Eq. 1 as 1/f (S).

$$f(S) = \frac{1}{-\log S} \quad . \quad . \quad . \quad . \quad . \quad . \quad . \quad . \quad . \quad . \quad . \quad . \quad . \quad . \quad (35)$$

Define the denominator of Eq. 33 as $1/\phi_m(S)$.

$$\phi_m(S) = \frac{1}{\sqrt{\frac{(1 - S)^3}{(1 + S)(S + P/h)(1 + P/h)}}} \quad . \quad . \quad . \quad . \quad . \quad . \quad . \quad . \quad (36)$$

A test of the relationship between f(S) and $\phi_m(S)$ can be made by assigning arbitrary values of S in Eq. 35 and values of S and P/h in Eq. 36.

The comparison between f(S), $\phi_m(S)$, and P/h is shown in Fig. 6. For P/h = 0, an equation between f(S) and $\phi_m(S)$ can be written

$$\phi_m(S) = 0.403\,[f(S)]^{1.50} \quad . \quad . \quad . \quad . \quad . \quad . \quad . \quad . \quad . \quad . \quad . \quad . \quad . \quad (37)$$

For P/h > 0, the lines of constant P/h for the logarithmic plot of Fig. 6 are curved. The lines of constant P/h have a constant slope of 1.50 when f(S) > 10. When f(S) = 10, the submergence is approximately 80 percent. As will be shown later in this report, submerged flow exists for the embankments under study when the submergence exceeds 85 or 86 percent [f(S) approximately equal to 15]. Consequently, for the purposes of this report, only the portions of the curves in Fig. 6 where f(S) > 15 are of importance. Therefore, a relationship similar to Eq. 37 can be written for each line of constant P/h in Fig. 6 for the portions of the curves where f(S) > 10. The actual relationship between f(S), $\phi_m(S)$, and P/h is not of great importance, but only the fact that a simple relationship does exist.

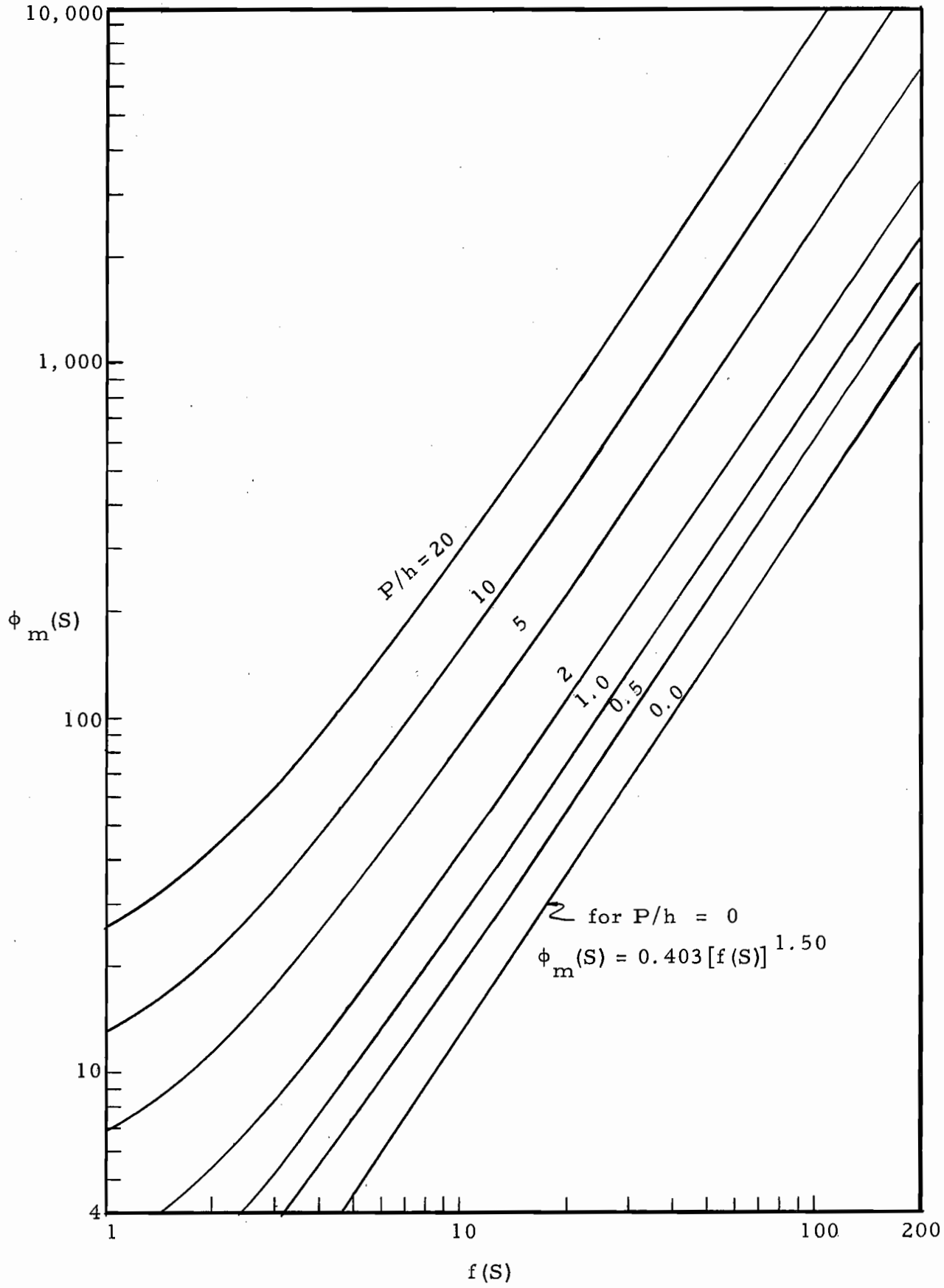

Fig. 6. Relationship between f(S), $\phi_m(S)$, and P/h for embankment-shaped weirs.

EXPERIMENTAL MODELS

The basic embankment design used in the study conducted by Kindsvater is illustrated in Fig. 7. The principal variables used to describe flow over an embankment are also illustrated by Fig. 7. The basic model was constructed at a 1:9 scale. In the original model, the intersections of the shoulder, embankment, and pavement surfaces were sharp and precise. Subsequent use and polishing rounded these intersections, but the results of Kindsvater (1964) gave no significant effects due to the rounding. The laboratory facilities were such that the discharge and degree of submergence could be controlled.

Throughout the study, scale-model tests were made on 17 variations of the basic embankment design. These tests were made by varying the hydraulic parameters given in Fig. 7 as well as testing various roughness elements. Typical variations are illustrated in Fig. 8. Fig. 8a is the basic embankment design illustrating the prototype dimensions. Figs. 8b, 8c, and 8d are variations used to test the effects of a rounded upstream shoulder, trip rod on the downstream shoulder, and berms on the embankment slopes, respectively.

Table 1, taken directly from Kindsvater (1964), contains the embankment design variations investigated in his study. All the models listed in Table 1 were constructed to a scale of 1:9. Corresponding to this construction scale, the unit-discharge, q, in the model is 1/27 of the discharge for the prototype embankment. The upstream flow depth,

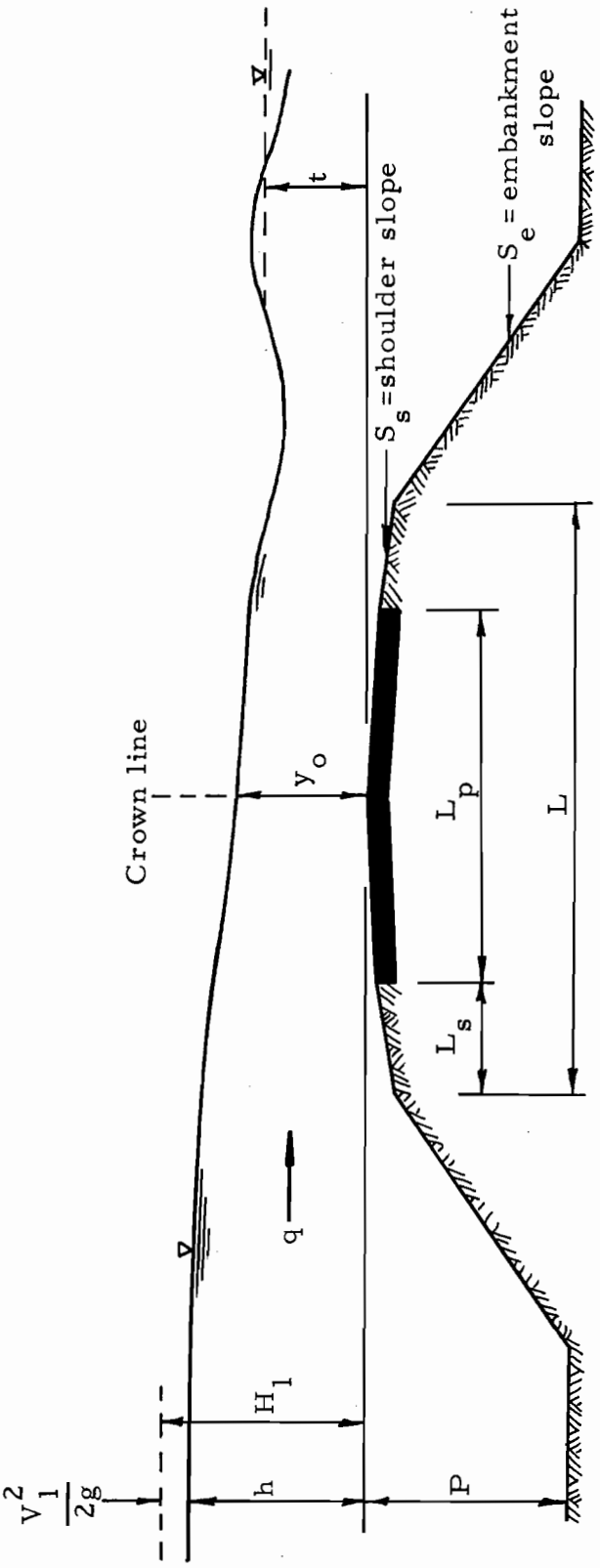

Fig. 7. Principal parameters describing flow over an embankment.

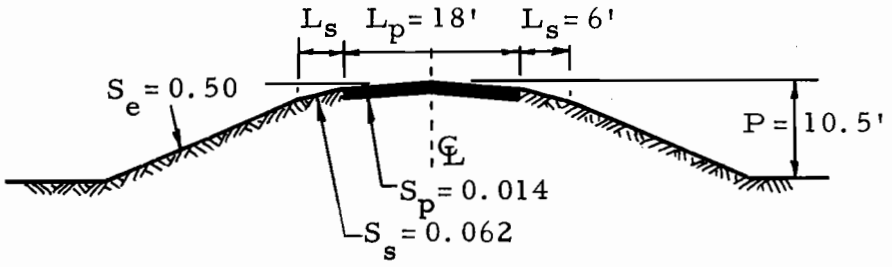

(a) Basic embankment design.

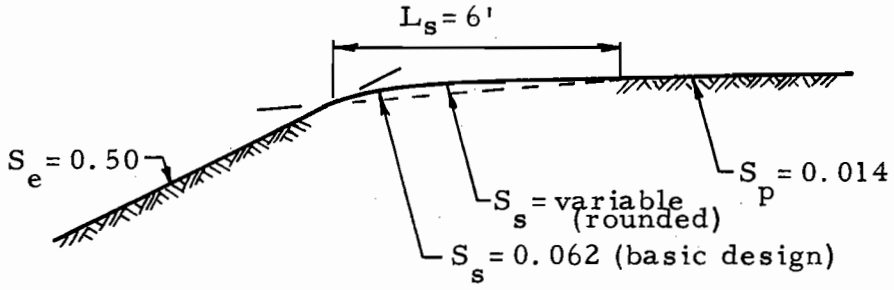

(b) Rounded upstream shoulder (Model K).

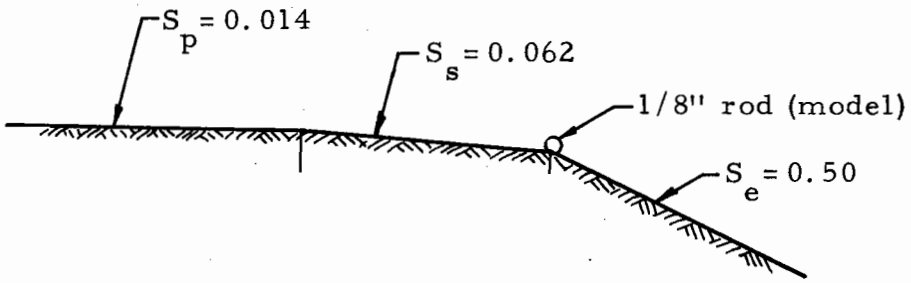

(c) Trip rod on the downstream shoulder (Model L).

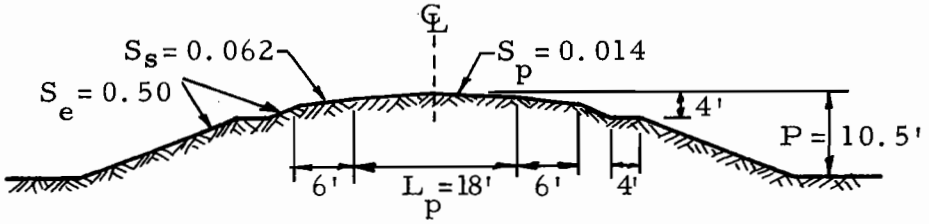

(d) Berms on the embankment slopes (Model M).

Fig. 8. Basic embankment design with some design variations (models K, L, and M).

Table 1. Summary of designs tested, 1:9-scale models.
[Asterisk (*) indicates that shape detail differs from basic design.]

Model	Investigator	Height, P (feet)		Pavement cross slope, S_p		Shoulder slope, S_s		Surface roughness	Remarks
		Prototype	Model	Inches: feet[1]	Nondimensional	Inches: feet[1]	Nondimensional		
A-1	Davidian	10.5	1.17	1.5:9	0.014	4.5:6	0.062	Smooth	Basic design
A-2	Prawel	10.5	1.17	1.5:9	.014	4.5:6	.062	do	do
A-3	do	10.5	1.17	1.5:9	.014	4.5:6	.062	do	do
A-4	Emmett	10.5	1.17	1.5:9	.014	4.5:6	.062	do	do
B	Prawel	*7.88	*.875	1.5:9	.014	4.5:6	.062	do	Effect of P
C	do	*5.25	*.583	1.5:9	.014	4.5:6	.062	do	do
D	do	*2.62	*.292	1.5:9	.014	4.5:6	.062	do	do
E	do	10.5	1.17	* 0:9	*.000	4.5:6	.062	do	Effect of S_p
F	do	10.5	1.17	* .9:9	*.008	4.5:6	.062	do	do
G	do	10.5	1.17	*2.2:9	*.020	4.5:6	.062	do	do
H	do	10.5	1.17	*2.8:9	*.026	4.5:6	.062	do	do
I	do	10.5	1.17	1.5:9	.014	*1.0:6	*.014	do	Effect of S_s
J	do	10.5	1.17	1.5:9	.014	*5.7:6	*.079	do	do
K-1	Davidian	10.5	1.17	1.5:9	.014	-----	----	do	(2)
K-2	Prawel	10.5	1.17	1.5:9	.014	-----	----	do	(2)
L	do	10.5	1.17	1.5:9	.014	4.5:6	.062	do	(3)
M	do	10.5	1.17	1.5:9	.014	4.5:6	.062	do	(4)
AA-1	Davidian	10.5	1.17	1.5:9	.014	4.5:6	.062	Window screen(all surfaces).	
AA-2	Emmett	10.5	1.17	1.5:9	.014	4.5:6	.062	do	
AB	do	10.5	1.17	1.5:9	.014	4.5:6	.062	Birdshot (except on pavement)	
AC	do	10.5	1.17	1.5:9	.014	4.5:6	.062	Birdshot (all surfaces).	
KA	Davidian	10.5	1.17	1.5:9	.014	-----	----	Window screen(all surfaces).	(2)

[1] Dimensions given in prototype units.
[2] Rounded transition between upstream embankment and shoulder surfaces.
[3] Trip sire on downstream edge of downstream shoulder.
[4] Berm on embankment slopes.

h, was measured at a prototype distance of approximately 52 feet upstream from the crown line, while the downstream depth, t, was measured at a prototype distance of 81 feet downstream from the crown line.

Model A, the basic design, is typical of the secondary asphaltic-pavement two-lane highways used in Georgia in 1947. Fig. 8a gives the details of model A. Further explanation of the embankment variations tested at Georgia Institute of Technology is given by Kindsvater (1964).

> Models A-1 through A-4 are different versions of the basic design. Each model represents a minor reconstruction of refurbishing which followed tests on some of the design variations. The purpose of models B, C, and D was to demonstrate the influence of h/P by comparison with model A. Thus, models otherwise identical with model A were tested with a full range of heads and with values of P equal to one-fourth, one-half, and three-fourths of the value of P for the basic design.
>
> To demonstrate the influence of pavement cross slope (S_p), models otherwise identical with model A were tested with 4 different values of S_p, 2 larger and 2 smaller than S_p for the basic design. Similarly, the influence of shoulder slope (S_s) was demonstrated with two models. For one of these, S_s was equal to S_p for model A. For the other, S_s was somewhat larger than S_s for the basic design.
>
> Model K was built especially for tests concerned with the influence of the boundary layer. It involved a rounded intersection between the upstream embankment slope and shoulder. Model L was identical with the basic design except for a tripwire located on the downstream edge of the downstream shoulder. Model M was designed to simulate the influence of the berm on both slopes of the embankment tested by Yarnell and Nagler (1930). Otherwise, model M was identical with model A. Details of design for models K, L, and M are given in Figs. 8b, 8c, and 8d.

Model A, the basis of comparison for all other designs, included smooth surfaces on all parts of the embankment and roadway. In terms of the prototype the characteristics revealed by this model are believed to simulate reasonably accurately the characteristics of a smooth, paved roadway in good repair.

Models AA and KA were rough-surfaced models. The roughness consisted of wire screen, a type of roughness used previously by Bauer (1954) in a related investigation. Uniform-flow tests made by Bauer, using a slightly different kind of screen, indicated that the effective roughness could be compared with rough concrete in the prototype.

Models AB and AC featured a relatively large, granular-type roughness, consisting of birdshot cemented to the surface in a random pattern. This variety of roughness is believed to simulate a reasonable maximum prototype roughness. For model AC the birdshot was applied to the entire model surface. For model AB the birdshot was applied only to the embankment slopes and shoulders. Model AB should give an indication of the influence of rough shoulders bordering a smooth pavement.

FREE FLOW EVALUATION

The discharge data available from Kindsvater's study was used for the free flow evaluation of the models listed in Table 1, except for models A-1, K-1, AA-1, and KA. The free flow data was plotted with q as the ordinate, and h, the upstream depth, as the abscissa on logarithmic paper. All of the plots resulted in straight lines with the data showing very little deviation. The equations resulting from these plots were of the form

$$q = C h^{n_1} \quad . \quad . \quad . \quad . \quad . \quad . \quad . \quad . \quad . \quad . \quad . \quad . \quad . \quad . \quad . \quad (38)$$

Table 2 lists the values of C and n_1 for the various models analyzed. As shown in Table 2, there is some variation in both the C and n_1 values for the various models. A discussion of the variations in the free flow equations will be made after analyzing the submerged flow data.

SUBMERGED FLOW EVALUATION

The submerged flow data for each model was plotted on logarithmic paper with the discharge per foot of length of embankment, q, as the ordinate, the change in water surface elevation, h - t, as the abscissa, and t/h, the submergence, as the varying parameter. Essentially, such plots are the graphical presentation of the submerged flow equation (Eq. 1). Typical of such plots are Figs. 9, 10, and 11. Fig. 9 is a plot of the data for model A-2, which is the basic embankment design, while the submerged flow data for model D has been plotted in Fig. 10, and Fig. 11 is a presentation of the data for model AB. Lines of constant submergence which best fit the data are drawn with a slope corresponding to the exponent of h in the free flow equation for the same model. For example, the constant submergence lines of 89.0, 93.7, 95.4, 96.4 97.5, and 98.5 percent have been drawn in Fig. 9 for model A-2. The slope of these lines of constant submergence is 1.53, which corresponds with the exponent of h in the free flow equation for model A-2 (Table 2).

The general submerged flow equation for each of the models is of the form

Table 2. Coefficients and exponents for model free flow equations.

Model	C	n_1
A-1	----	----
A-2	3.19	1.53
A-3	3.19	1.53
A-4	3.19	1.53
B	3.25	1.53
C	3.43	1.56
D	3.62	1.59
E	3.24	1.54
F	3.24	1.54
G	3.24	1.54
H	3.24	1.54
I	3.24	1.54
J	3.24	1.54
K-1	----	----
K-2	3.24	1.54
L	3.24	1.55
M	3.21	1.52
AA-1	----	----
AA-2	3.22	1.56
AB	3.17	1.53
AC	3.15	1.55
KA	----	----

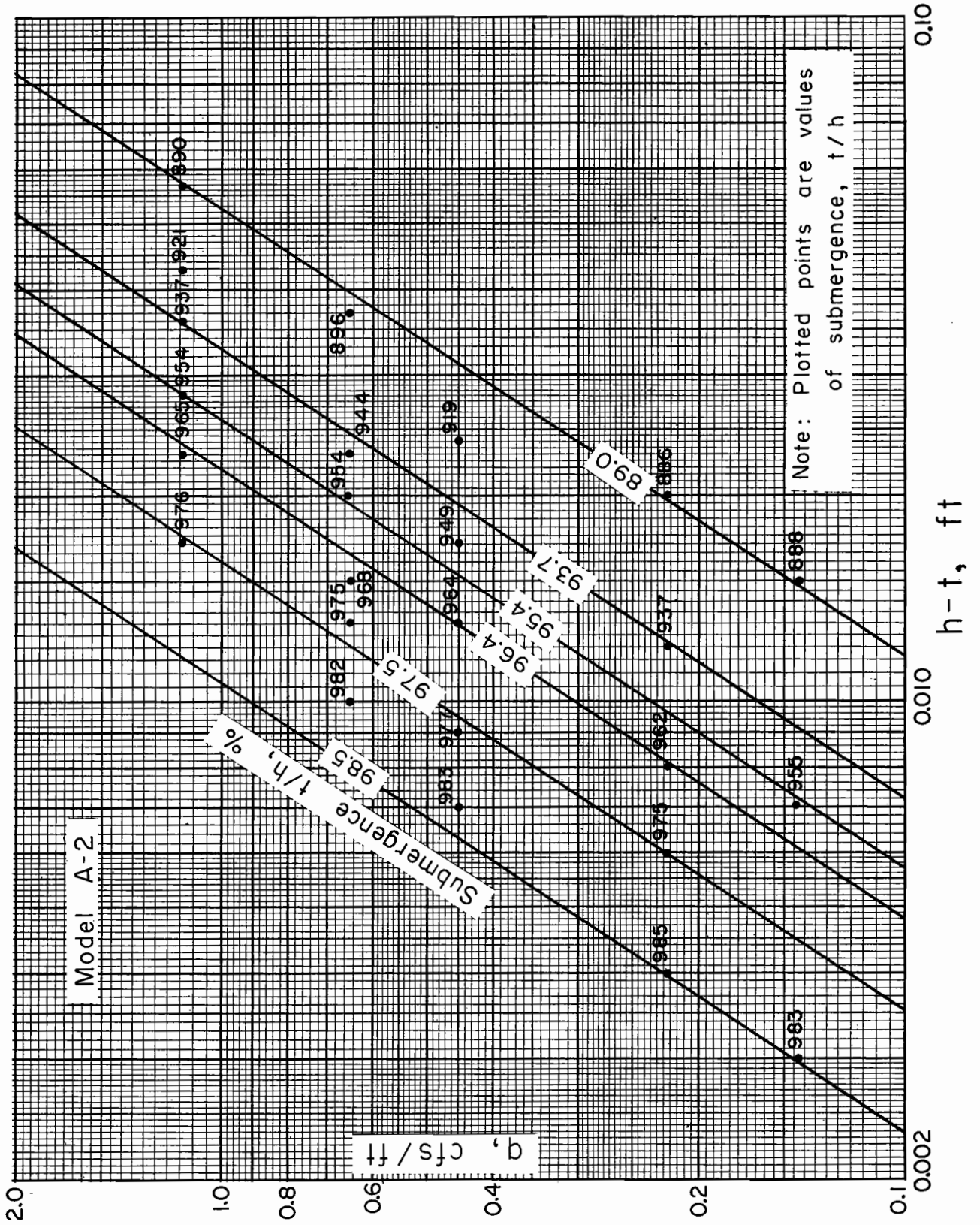

Fig. 9. Plot of submerged flow data for model A-2.

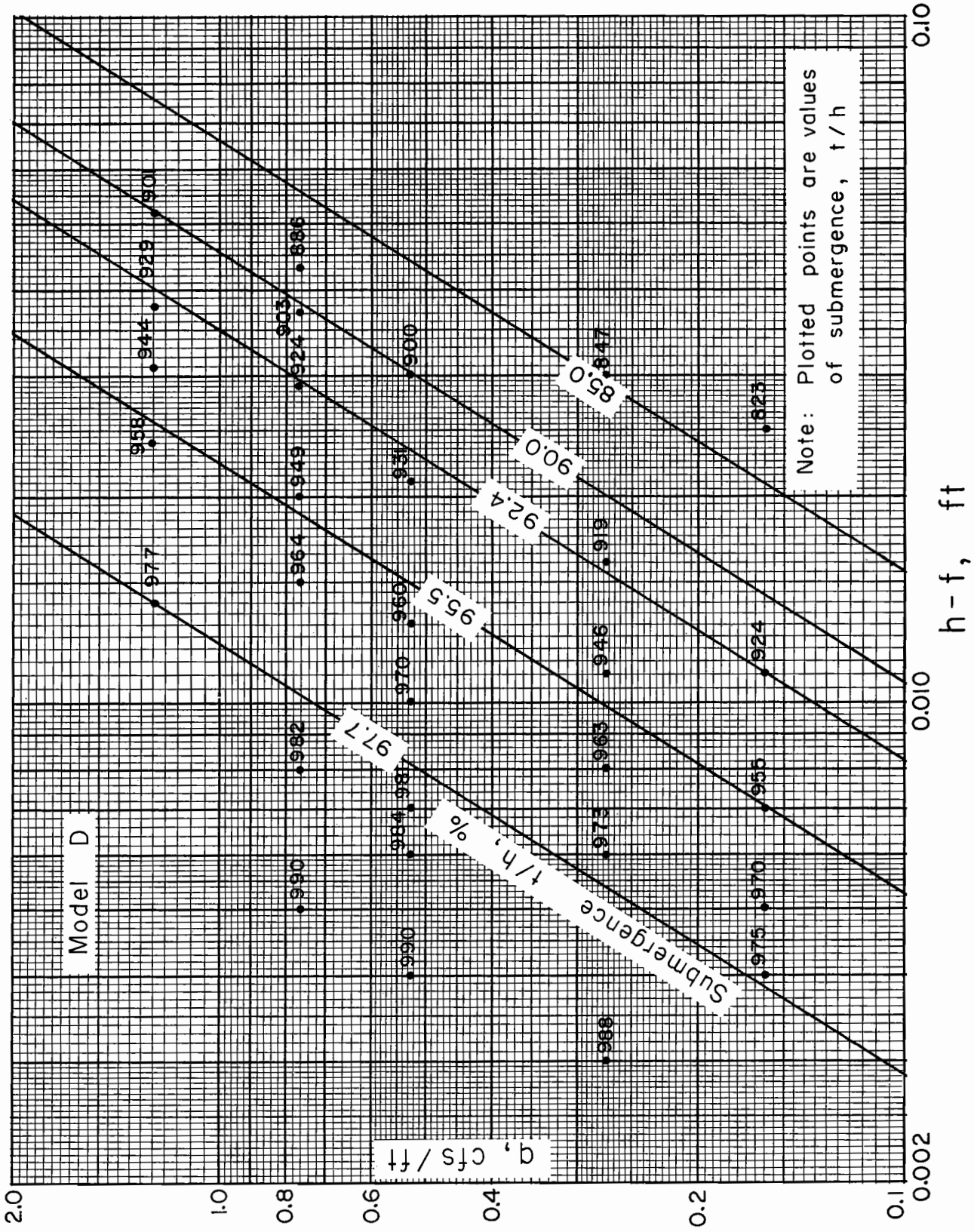

Fig. 10. Plot of submerged flow data for model D.

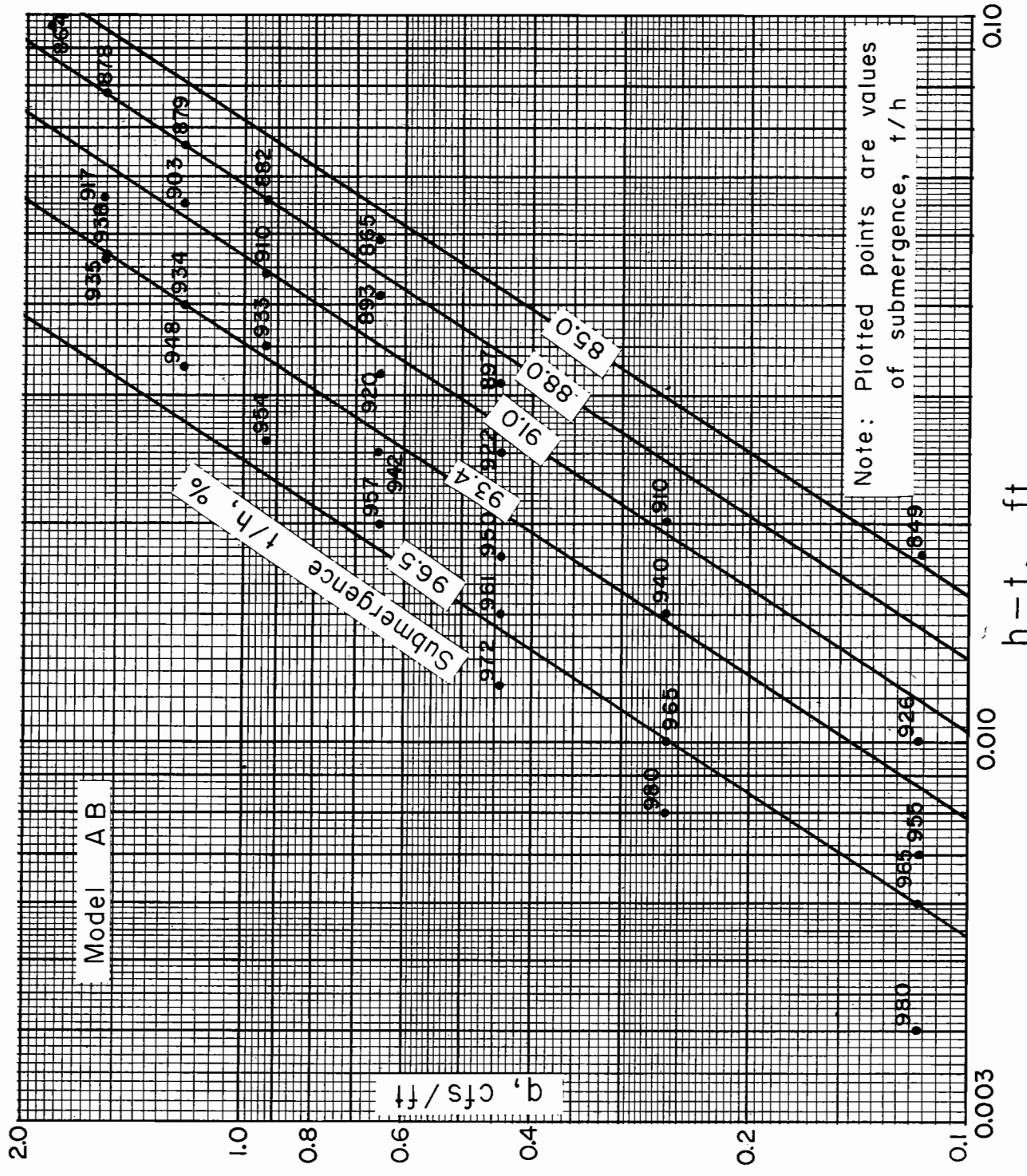

Fig. 11. Plot of submerged flow data for model AB.

$$q = \frac{C_1 (h - t)^{n_1}}{(-\log t/h)^{n_2}} \quad . \quad . \quad . \quad . \quad . \quad . \quad . \quad . \quad . \quad . \quad . \quad . \quad (39)$$

The values of C_1, n_1, and n_2 for the various models are summarized in Table 3. As an example, the submerged flow equation for model A-2 is

$$q = \frac{2.41 (h - t)^{1.53}}{(-\log t/h)^{1.20}} \quad . \quad . \quad . \quad . \quad . \quad . \quad . \quad . \quad . \quad . \quad . \quad . \quad (40)$$

The model A-2 data has been converted to prototype data from which an equation for the prototype structure was developed and then plotted in Fig. 12. Thus, Fig. 12 becomes the field rating curves for a highway embankment similar in form to the basic structure studied by Kindsvater (model A).

The transition submergence, S_t, is defined as the value of submergence, t/h, at which free flow changes to submerged flow (supercritical flow changes to subcritical flow). In essence, the transition signifies that the Froude number is equal to one at a single flow cross-section, and for every other cross-section the Froude number is less than one. At the transition from free flow to submerged flow, the discharge equations for the two flow conditions should be equal. Consequently, if the discharge equations are known, the transition submergence can be obtained by setting the free and submerged flow equations equal to one another. To illustrate the solution for the transition submergence, the free flow and submerged flow discharge equations for model A-2 will be equated.

Table 3. Coefficients and exponents for model submerged flow equations.

Model	C_1	n_1	n_2	S_t, % (from eqs.)	S_t, % (rounded)
A-1	----	----	----	----	--
A-2	2.41	1.53	1.20	84.9	85
A-3	2.41	1.53	1.20	84.9	85
A-4	2.41	1.53	1.20	84.9	85
B	2.35	1.53	1.23	85.3	85
C	2.09	1.56	1.32	86.0	86
D	1.98	1.59	1.37	86.0	86
E	2.01	1.54	1.28	85.0	85
F	2.01	1.54	1.28	85.0	85
G	2.01	1.54	1.28	85.0	85
H	2.01	1.54	1.28	85.0	85
I	2.01	1.54	1.28	85.0	85
J	2.01	1.54	1.28	85.0	85
K-1	----	----	----	----	--
K-2	2.01	1.54	1.28	85.0	85
L	2.54	1.55	1.20	85.2	85
M	1.96	1.52	1.28	86.0	86
AA-1	----	----	----	----	--
AA-2	2.34	1.56	1.23	84.0	84
AB	2.24	1.53	1.22	84.2	84
AC	2.31	1.55	1.22	84.9	85
KA	----	----	----	----	--

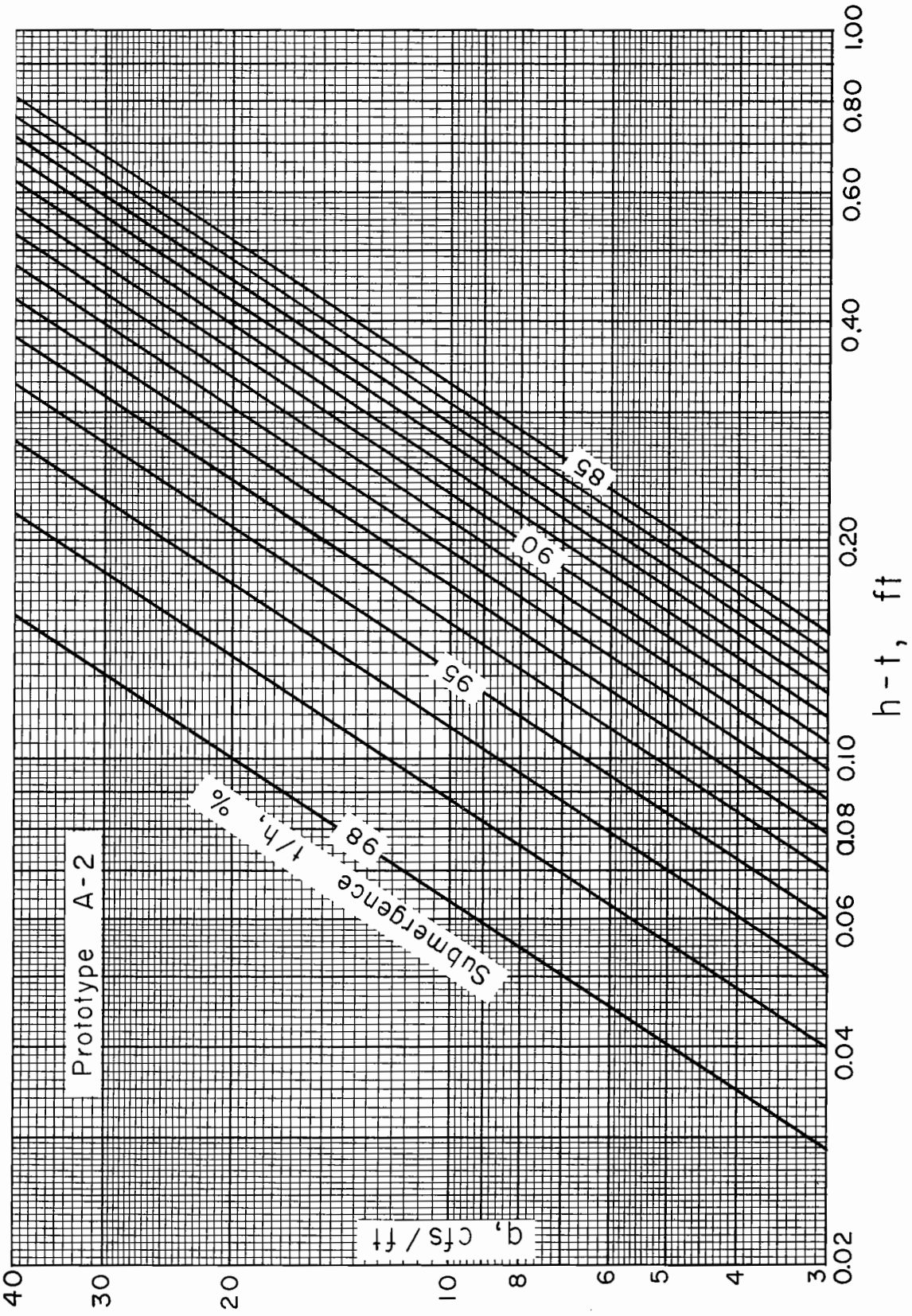

Fig. 12. Submerged flow calibration curves for basic prototype embankment design.

$$\frac{2.41\ (h - t)^{1.53}}{(-\log t/h)^{1.20}} = 3.19\ h^{1.53}$$

$$\frac{2.41\ (h - t)^{1.53}}{3.19\ h^{1.53}} = (-\log t/h)^{1.20}$$

$$0.755\ (1 - t/h)^{1.53} = (-\log t/h)^{1.20}$$

A solution is obtained by trial and error.

$$t/h = S_t = 0.849 = 84.9\%$$

Kindsvater (1964) states that the value of the transition (incipient) submergence determined by his study is about 84 percent. The transition submergence given by Kindsvater is based on the downstream flow depth, t, divided by the total upstream head, H_1 (upstream flow depth plus velocity head), whereas the value cited by the authors (85%) is based on the ratio of the downstream flow depth divided by the upstream flow depth (t/h). The transition submergence will naturally be greater when computed from the ratio, t/h, as compared with the ratio, t/H_1.

The transition submergence value derived from the discharge equations for each of the models is listed in Table 3. These transition submergence values range from 84 to 86 percent. Such a narrow range of values is surprising because the magnitude of the transition submergence is very sensitive to changes in the coefficients or exponents of the discharge equations. The excellent accuracy in the computation of the transition submergence for each model again points out the quality of the data developed by Kindsvater.

EFFECTS OF EMBANKMENT FORM

The effects of varying the geometry in the different models will be compared with the A models (models A-2, A-3, and A-4), which are considered the basic embankment design in this study. Primarily, the information being compared is the variation in embankment geometry (Table 1), the coefficients and exponents in the free flow equations (Table 2), and the coefficients and exponents in the submerged flow equations (Table 3).

Models B, C, and D were studied to illustrate the effect of embankment height on the discharge equations. The effects of embankment height on the discharge characteristics of flow over a highway embankment can be evaluated by comparing the coefficients and exponents in Tables 2 and 3. The submerged flow coefficient, C_1, varies from 2.41 in the A models to 1.98 in model D. The value of n_2 increases from 1.20 in the A models to 1.23 in model B, 1.32 in model C, and 1.37 in model D. The fact that the embankment height has a marked and definite effect on the discharge relationship is readily apparent. A comparison between the A models and model B, using the extreme fluctuations in flow depths which could actually occur, results in the discharge, q, being 2 to 11 percent greater in model B. For similar extreme fluctuations in flow depth, model C would result in flow rates as much as 26 percent greater than the A models, while the discharge over model D would vary from 10 percent smaller to 32 percent greater

than the A models. The effect of embankment height is illustrated in Fig. 13 for submergences of 85 and 98 percent. The 85 percent submergence line was chosen because it represents the transition submergence. Essentially, the variation in the 85 percent submergence lines represents the differences in the free flow equations for the models. The differences in the 98 percent submergence lines illustrate the condition of nearly maximum variation between the models.

Models E, F, G, H, I, J, K-1, and K-2 were constructed to evaluate the effects of pavement slope, S_p, and shoulder slope, S_s, on the discharge characteristics of embankment-shaped weirs. The discharge equations for models E, F, G, H, I, J, and K-2 are identical. The submerged flow coefficient, has a value of 2.01 for these models as compared with 2.41 for the A models. The value of the submerged flow exponent, n_2, varies from 1.20 for the A models to 1.28 for the models used to test the effect of pavement slope and shoulder slope. Fig. 14, which is similar in nature to Fig. 13, illustrates the differences between the A models and the E, F, G, H, I, J, K-2, L, and M models. Again, the 85 percent and 98 percent submergence lines have been used to portray the differences at a high submergence and the transition submergence, which is comparable to the free flow equations. These differences could result in a discharge which varies from 4 percent less to 13 percent greater than the discharge through model A-2.

Model L is different from the basic model only in that it has a trip wire on the downstream edge of the downstream shoulder (Fig. 8c).

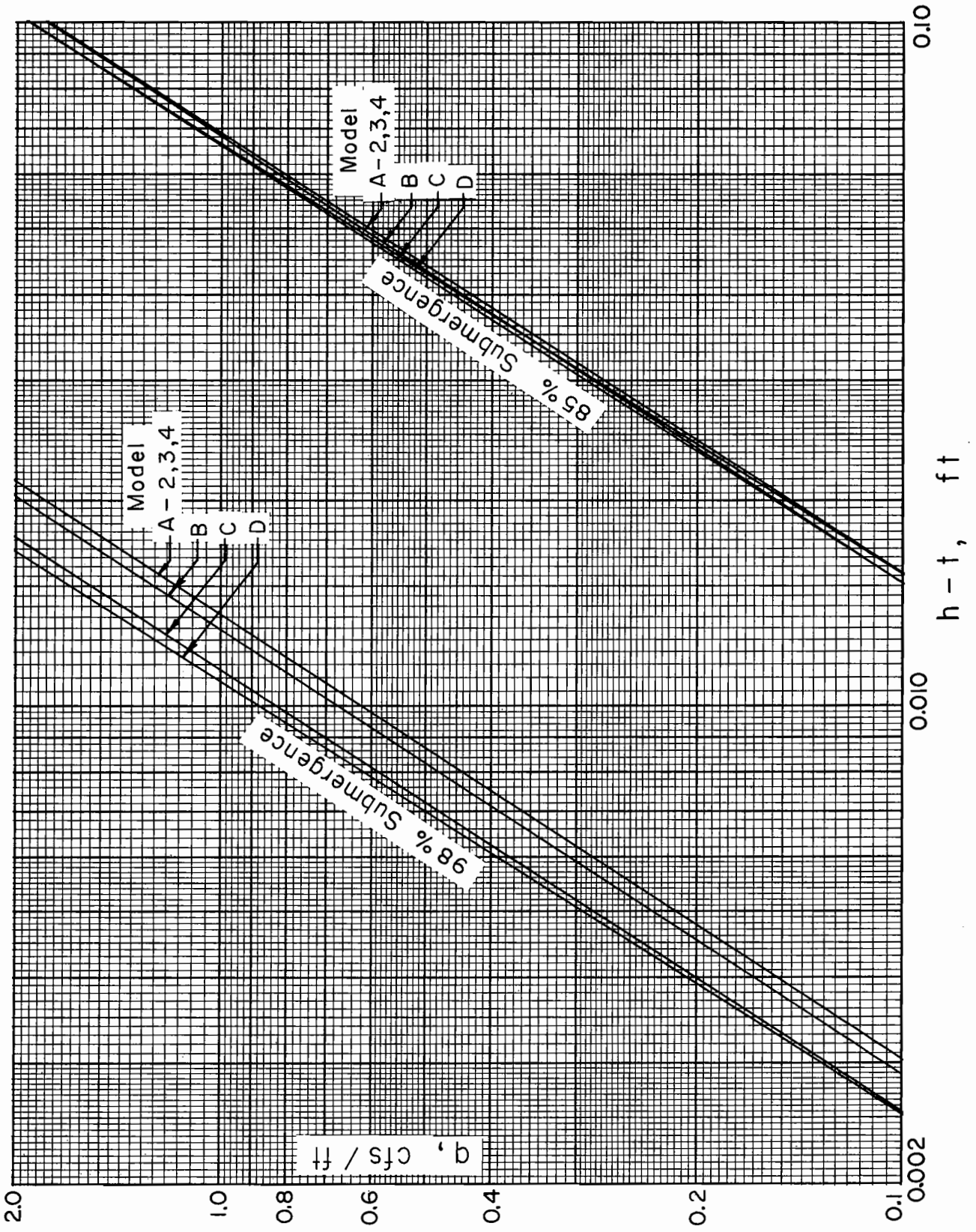

Fig. 13. Plot of 85 and 98 percent submergence lines illustrating the differences in the basic model design and models B, C, and D.

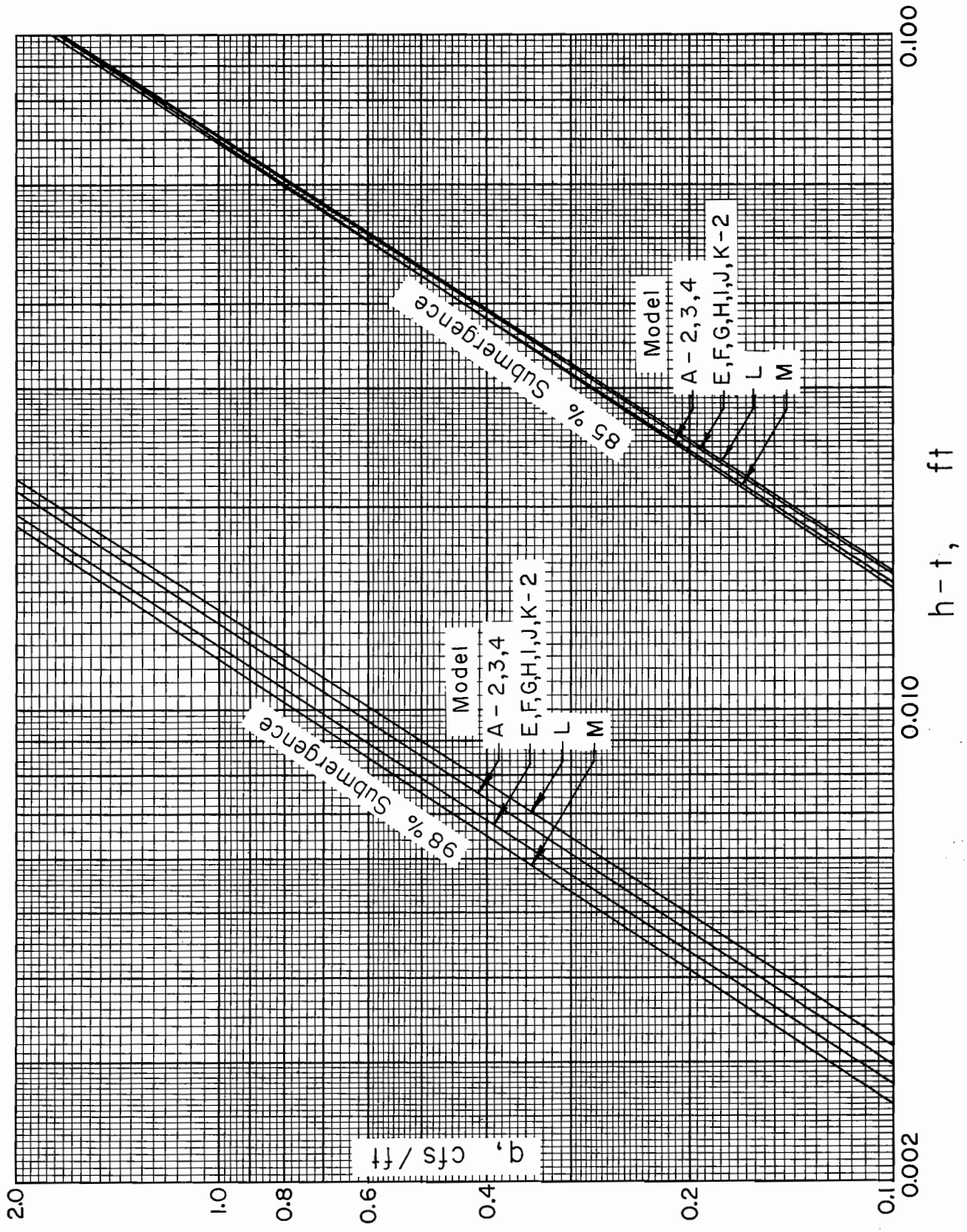

Fig. 14. Plot of 85 and 98 percent submergence lines illustrating the differences in the basic model design and models E, F, G, H, I, J, K-2, L, and M.

The equations which describe the discharge through model L vary little from those describing the flow in the basic model. Actually, in the extreme cases of flow depths, the discharge would only be about 5 percent less in model L. This could indicate that the trip wire may act in a manner which increases the submergence of the flow.

Model M differs in geometry from the A models in that berms have been constructed on the embankment slopes (Fig. 8d). The berms have an effect on the discharge over the model as compared with the basic model embankment. The submerged flow coefficient, C_1, is much less and the submergence exponent, n_2, much greater in model M than in model A-2. Under extreme flow conditions, the discharge over model M could be 16 percent greater than the flow over model A-2.

EFFECTS OF EMBANKMENT ROUGHNESS

Models AA-2, AB, and AC were constructed to evaluate the effect of roughness. The models were roughened either by birdshot or window screen. Model AA-2 had a screen-wire roughness on all surfaces. Such a roughness should be comparable to a dirt road. Both the exponent of the change in water surface elevation, n_1, and the submergence exponent, n_2, for model AA-2 are greater in value than exponents for the basic embankment model. Further evaluation discloses that the discharge over model AA-2 will be 2 to 14 percent lower than the flow over model A-2.

Models AB and AC had birdshot (No. 9 with 0.080-inch diameter) glued to their surfaces. Model AC had birdshot placed on all surfaces while model AB did not have birdshot placed on the pavement. Hence, model AB would be analogous to an asphalted road with gravel placed on the shoulders and embankment slopes, whereas model AC would be considered comparable to a gravel road constructed with 3/4-inch diameter stone. A difference exists in the discharge equations for models AB and AC. Model AB gives discharge values which are 2 percent lower to 4 percent greater than the basic embankment model, whereas model AC yields discharges which vary from 3 to 11 percent less than the basic model. Also, model AC gives flow rates which are less than the flows passing over model AB. Consequently, the increased roughness on the pavement does have a significant effect in retarding the flow.

Fig. 15 graphically illustrates the differences in the discharge equations for the basic embankment model and models used to test the effects of surface roughness (models AA-2, AB, and AC). For a given set of flow depths (h and t), the discharge passing over models AA-2, AB, and AC is always less than the discharge passing over the basic embankment model (A models). Therefore, the surface roughness does have an effect on the stage-fall-discharge relations for an embankment-shaped weir.

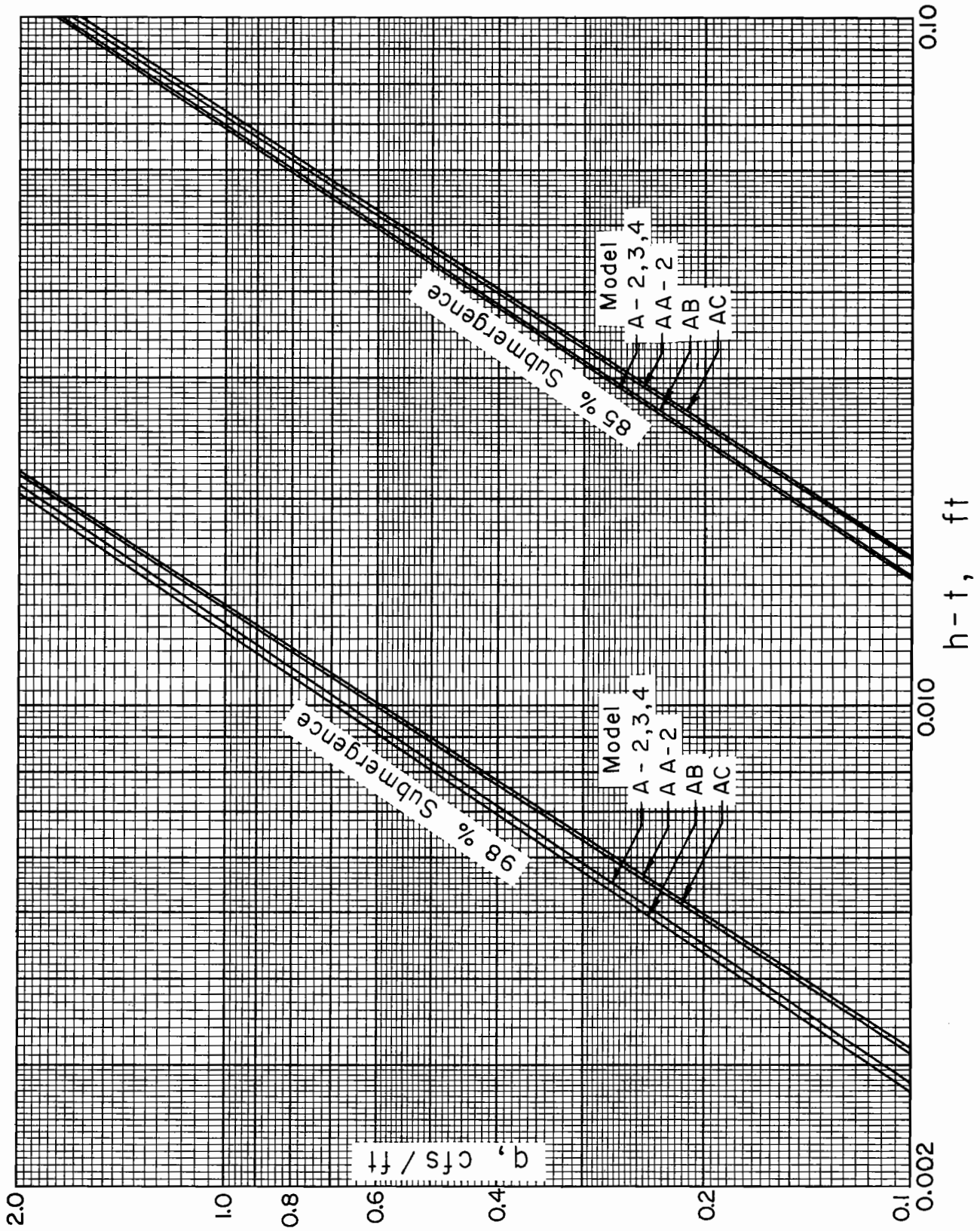

Fig. 15. Plot of 85 and 98 percent submergence lines illustrating the differences in the basic model design and models AA-2, AB, and AC.

SIGNIFICANCE OF STUDY

An analytical method of evaluating submerged flow over an embankment-shaped weir has been illustrated. The method of analysis is an extension of the authors earlier efforts regarding side contractions (flumes) in open channels. Since the submerged flow analysis has worked very well for embankment-shaped weirs, there is no reason to believe that it would not work for other weir forms. The analytical techniques employed have demonstrated that the surface roughness of the embankment-shaped weir does have a significant effect on the stage-fall-discharge relation.

REFERENCES

Bauer, W. J. 1954. Turbulent boundary layer on steep slopes. Transactions, ASCE, Vol. 119, p. 1212.

Hyatt, M. Leon. 1965. Design, calibration, and evaluation of a trapezoidal measuring flume by model study. M. S. Thesis, Utah State University, Logan, Utah. March.

Hyatt, M. L., G. V. Skogerboe, and K. O. Eggleston. 1966. Laboratory investigations of submerged flow in selected Parshall flumes. Report PR-WR6-6, Utah Water Research Laboratory, College of Engineering, Utah State University, Logan, Utah. January.

Kindsvater, Carl E. 1964. Discharge characteristics of embankment-shaped weirs. Geological Survey Water-Supply Paper 1617-A. U. S. Geological Survey and Georgia Institute of Technology.

Skogerboe, G. V., W. R. Walker, and L. R. Robinson. 1965. Design, operation, and calibration of the Canal A submerged rectangular measuring flume. Report PR-WG24-3, Utah Water Research Laboratory, College of Engineering, Utah State University, Logan, Utah. March.

Skogerboe, G. V., M. L. Hyatt, J. R. Johnson, and J. D. England. 1965. Submerged Parshall flumes of small size. Report PR-WR6-1, Utah Water Research Laboratory, College of Engineering, Utah State University, Logan, Utah. July.

Skogerboe, G. V., M. L. Hyatt, J. D. England, and J. R. Johnson. 1965. Submergence in a two-foot Parshall flume. Report PR-WR6-2, Utah Water Research Laboratory, College of Engineering, Utah State University, Logan, Utah. August.

Yarnell, D. L., and Nagler, F. A. 1930. Flow of flood water over railway and highway embankments. Public Roads, Vol. 11, No. 2, April, p. 30-34.